CrystEngComm

RSC Publishing

PAPER

View Article Online
View Journal | View Issue

Cite this: *CrystEngComm*, 2013, **15**, 3630

Seven structural versatile coordination polymers based on a flexible bis(triazole) and polycarboxylate co-ligands: syntheses, structures and properties†

Min Li, Qian Ling, Zhi Yang, Bao-Long Li* and Hai-Yan Li

Received 10th January 2013,
Accepted 26th February 2013

DOI: 10.1039/c3ce00057e

www.rsc.org/crystengcomm

Seven coordination polymers $\{[Mn(tmtz)_{0.5}(OH\text{-}bdc)(H_2O)_2]\cdot 2.75H_2O\}_n$ (**1**), $[Mn(tmtz)_{1.5}(1,3\text{-}bdc)]_n$ (**2**), $[Mn(tmtz)(1,4\text{-}bdc)]_n$ (**3**), $[Co(tmtz)(oba)]_n$ (**4**), $\{[Co_4(tmtz)_2(bptc)_2(H_2O)_7]\cdot 3.5H_2O\}_n$ (**5**), $\{[Ni(tmtz)_{1.5}(1,3\text{-}bdc)]\cdot 0.5H_2O\}_n$ (**6**), $[Ni(tmtz)(oba)(H_2O)]_n$ (**7**) (tmtz = 1,4-bis(1,2,4-triazol-1-ylmethyl)-2,3,5,6-tetramethylbenzene, OH-bdc = 5-hydroxy-1,3-benzenedicarboxylate, 1,3-bdc = 1,3-benzenedicarboxylate, 1,4-bdc = 1,4-benzenedicarboxylate, H_2oba = 4,4′-oxybis(benzoic acid), bptc = 3,3′,4,4′-benzophenonetetracarboxylate) have been synthesized and structurally characterized. **1** exhibits a 1D ladder structure and a 3D supramolecular architecture. **2** and **6** have similar 5-connected 2D networks through the 1,3-bdc ligand connecting $[M(tmtz)_{1.5}]_n$ 1D ladders, with the point symbol $(4^8\cdot 6^2)$. **3** has a (4,6)-connected 3D fsc network with a point symbol of $(4^4\cdot 6^2)(4^4\cdot 6^{10}\cdot 8)$. **4** shows a 1D tubular-like chain. **5** exhibits a complicated (3,4,4)-connected 3D network with a point symbol of $(4\cdot 10\cdot 12)_2(4\cdot 8^3\cdot 10\cdot 12)_2(8^2\cdot 10^2\cdot 12^2)$. Such a (3,4,4)-connected 3D network is unprecedented to the best of our knowledge. **7** displays a 2D (4,4) network which crystallizes in the chiral orthorhombic space group $P2_12_12_1$. The results indicate that the central metal ions, polycarboxylate and flexible triazole co-ligands have a great effect on the formation and the structures of the coordination polymers. The thermal stability and luminescence were investigated. The crystal structures and solid-state circular dichroism (CD) spectra measurements confirmed the occurrence of the spontaneous resolution of **7** and demonstrated that the resulting crystal of **7** is a racemic mixture.

Introduction

The design and construction of metal–organic frameworks (MOFs) are motivated by their potential applications as functional materials in fields such as gas storage, chemical separation, catalysis, luminescence and their intriguing variety of topologies.[1] To design and synthesize MOFs with a unique structural diversity, it would be highly desirable to choose organic ligands with ideal coordination modes. Flexible bidentate N-donor ligands, such as bis(imidazole)[2] and bis(triazole)[3] ligands, are widely used to construct coordination polymers because flexible ligands can adopt different conformations according to the geometric needs of the different metal ions. In previous work, we synthesized a lot of coordination polymers using flexible bis-triazole building blocks, such as 1,2-bis(1,2,4-triazol-1-yl) ethane (bte),[4] 1,2-bis(1,2,4-triazol-4-yl) ethane (btre),[5] 1,3-bis(1,2,4-triazol-1-yl)propane (btp),[6] 1,4-bis(1,2,4-triazol-1-yl)butane (btb)[7] and 1,4-bis(1,2,4-triazol-1-ylmethyl)benzene (bbtz).[8] At present, we are focusing our attention on using a new flexible 1,4-bis(1,2,4-triazol-1-ylmethyl)-2,3,5,6-tetramethylbenzene ligand (tmtz, Scheme 1), which has four methyl substitutes for the bbtz ligand, as the main ligand to construct new coordination polymers based mostly on the following considerations: (1)

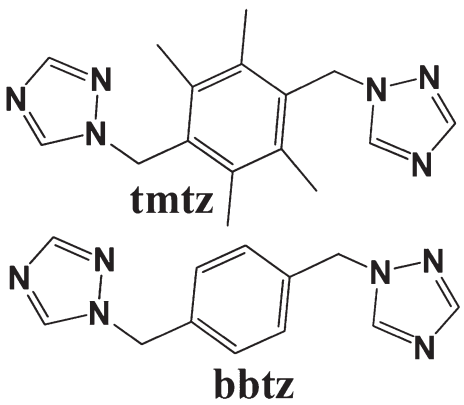

Scheme 1 The tmtz and bbtz ligands.

Key Laboratory of Organic Synthesis of Jiangsu Province, College of Chemistry, Chemical Engineering and Materials Science, Soochow University, Suzhou 215123, P. R. China. E-mail: libaolong@suda.edu.cn

† Electronic supplementary information (ESI) available: Selected bond lengths and angles, hydrogen bonding, additional figures for the crystal structures and TGA. CCDC 917534–917540, 926060. For ESI and crystallographic data in CIF or other electronic format see DOI: 10.1039/c3ce00057e

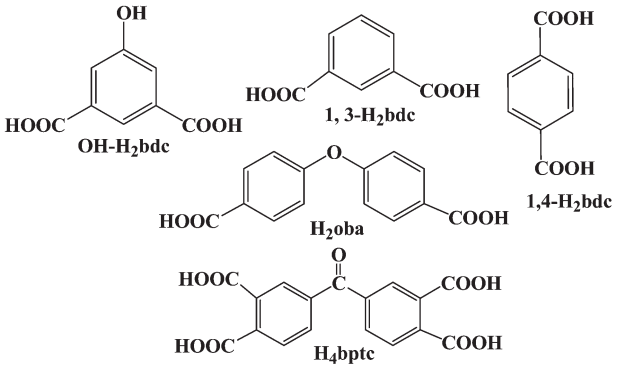

Scheme 2 The polycarboxylate ligands in this work.

two triazole groups can freely twist around two $-CH_2-$ groups with different angles to generate different conformations and coordination modes. (2) Four methyl groups have steric hindrance and electron giving ability and can play the role of the coordination modes of triazole groups. (3) The aromatic rings may form strong π···π stacking interactions and may lead to variable π···π interactions modes and architectures.

Organic polycarboxylate ligands (Scheme 2) have been widely used in synthesizing porous MOFs with various coordination modes of the carboxyl group.[9] In the present work, we have successfully synthesized seven new coordination polymers based on the flexible ligand tmtz, namely, $\{[Mn(tmtz)_{0.5}(OH\text{-}bdc)(H_2O)_2]\cdot 2.75H_2O\}_n$ (**1**), $[Mn(tmtz)_{1.5}(1,3\text{-}bdc)]_n$ (**2**), $[Mn(tmtz)(1,4\text{-}bdc)]_n$ (**3**), $[Co(tmtz)(oba]_n$ (**4**), $\{[Co_4(tmtz)_2(bptc)_2(H_2O)_7]\cdot 3.5H_2O\}_n$ (**5**), $\{[Ni(tmtz)_{1.5}(1,3\text{-}bdc)]\cdot 0.5H_2O\}_n$ (**6**), $[Ni(tmtz)(oba)(H_2O)]_n$ (**7**) (tmtz = 1,4-bis(1,2,4-triazol-1-ylmethyl)-2,3,5,6-tetramethylbenzene, OH-bdc = 5-hydroxy-1,3-benzenedicarboxylate, 1,3-bdc = 1,3-benzenedicarboxylate, 1,4-bdc = 1,4-benzenedicarboxylate, H_2oba = 4,4′-oxybis(benzoic acid), bptc = 3,3′,4,4′-benzophenonetetracarboxylate). The crystal structures are presented and discussed. Furthermore, the thermal stability and the luminescence have been investigated. The crystal structures and solid-state circular dichroism (CD) spectra measurements confirmed the occurrence of the spontaneous resolution of **7** and demonstrated that the resulting crystal of **7** is a racemic mixture.

Experimental section

Materials and physical measurements

All the reagents were of analytical grade and used without further purification. The ligand tmtz was synthesized according to the literature method.[10] Elemental analyses for C, H and N were performed on a Perkin-Elmer 240C analyser. IR spectra were obtained for KBr pellets on a Nicolet 170SX FT-IR spectrophotometer in the 4000–400 cm^{-1} region. The luminescence measurements were carried out in the solid state at room temperature and the spectra were collected with a Perkin-Elmer LS50B spectrofluorimeter. TGA was carried out using a Thermal Analyst 2100 TA Instrument and an SDT 2960 Simultaneous TGA-DTA Instrument in flowing dinitrogen at a heating rate of 10 °C min^{-1}. The solid-state circular dichroism (CD) spectra were recorded on an Aviv model 410 spectropolarimeter (Lakewood, New Jersey, USA) with KBr pellets.

Synthesis of $\{[Mn(tmtz)_{0.5}(OH\text{-}bdc)(H_2O)_2]\cdot 2.75H_2O\}_n$ (1)

$Mn(NO_3)_2\cdot 4H_2O$ (0.025 g, 0.10 mmol) was added into a solution of tmtz (0.030 g, 0.10 mmol) and OH-H_2bdc (0.021 g, 0.10 mmol) in CH_3OH (5 mL) and H_2O (10 mL), which was adjusted to pH 7 with a dilute NaOH solution. The resultant solution was continuously stirred for 20 minutes and filtered. The filtrate was kept at room temperature and a few days later colorless crystals of **1** were obtained with a yield of 31% (based on tmtz). Anal. Calcd for $C_{16}H_{23.5}MnN_3O_{9.75}$: C, 40.99; H, 5.05; N, 8.97 Found: C, 40.78; H, 5.07; N, 8.90. IR (cm^{-1}, KBr): 3907w, 3536w, 3142m, 1623m, 1553s, 1442m, 1399s, 1312w, 1277m, 1229w, 1141m, 1019w, 984m, 892m, 816w, 783m, 736m, 677m.

Synthesis of $[Mn(tmtz)_{1.5}(1,3\text{-}bdc)]_n$ (2)

A 10 mL CH_3OH solution of tmtz (0.030 g, 0.10 mmol) and 1,3-H_2bdc (0.017 g, 0.10 mmol) was carefully layered over an aqueous solution (10 mL) of $Mn(NO_3)_2\cdot 4H_2O$ (0.025 g, 0.10 mmol) in a test tube. Colorless single crystals of **2** were obtained in a 65% yield after the mixture was allowed to stand at room temperature for two weeks (based on tmtz). Anal. Calcd for $C_{32}H_{34}MnN_9O_4$: C, 57.92; H, 5.16; N, 19.00. Found: C, 57.87; H, 5.13; N, 19.02. IR (cm^{-1}, KBr): 3483w, 3132w, 1641m, 1606s, 1554s, 1480w, 1383s, 1272m, 1206w, 1128m, 1006w, 980w, 828w, 741m, 720m, 674m.

Synthesis of $[Mn(tmtz)(1,4\text{-}bdc)]_n$ (3)

The synthetic procedure was similar to that of **2** except that 1,3-H_2bdc (0.017g, 0.10 mmol) was replaced by 1,4-H_2bdc (0.017 g, 0.10 mmol). Colorless crystals of **3** were obtained after about two weeks in a 55% yield (based on tmtz). Anal. Calcd. for $C_{24}H_{24}MnN_6O_4$: C, 55.93; H, 4.69; N, 16.31. Found: C, 55.89; H, 4.67; N, 16.27. IR (cm^{-1}, KBr): 3404w, 3105w, 1639m, 1573s, 1520w, 1381s, 1310w, 1269m, 1137m, 1018w, 979m, 871w, 807m, 753s, 679m, 651w, 497m.

Synthesis of $[Co(tmtz)(oba]_n$ (4)

Tmtz (0.030 g, 0.10 mmol), $Co(NO_3)_2\cdot 6H_2O$ (0.029 g, 0.10 mmol) and H_2oba (0.026 g, 0.10 mmol) in CH_3OH (5 mL) and H_2O (10 mL) was adjusted to pH 6 with a dilute NaOH solution. The mixture was placed in a Teflon-lined stainless steel vessel and was sealed and heated to 110 °C for 24 h, followed by cooling to room temperature at 5 °C h^{-1}. Pink crystals of **4** were obtained with a yield of 48% based on tmtz. Anal. Calcd for $C_{30}H_{28}CoN_6O_5$: C, 58.92; H, 4.62; N, 13.75. Found: C, 58.86; H, 4.64; N, 13.72. IR (cm^{-1}, KBr): 3472W, 3088w, 1592s, 1530s, 1389s, 1274m, 1219s, 1157m, 1132m, 1091w, 1009w, 984w, 872m, 822w, 780m, 678m, 655m.

Synthesis of $\{[Co_4(tmtz)_2(bptc)_2(H_2O)_7]\cdot 3.5H_2O\}_n$ (5)

The synthetic procedure was similar to that of **4** except that H_2oba (0.026 g, 0.10 mmol) was replaced by H_4bptc (0.036g, 0.10 mmol). Pink crystals of **5** were obtained with a yield of

34% based on tmtz. Anal. Calcd for $C_{66}H_{73}Co_4N_{12}O_{28.5}$: C, 45.93; H, 4.26; N, 9.74. Found: C, 45.95; H, 4.23; N, 9.68. IR (cm^{-1}, KBr): 3770w, 3470~2940w, 1673m, 1613s, 1572s, 1487m, 1438m, 1390s, 1303w, 1274m, 1238m, 1200w, 1130m, 1088w, 1004w, 984w, 850w, 803w, 760m, 676m.

Synthesis of $\{[Ni(tmtz)_{1.5}(1,3\text{-bdc})]\cdot 0.5H_2O\}_n$ (6)

A mixture of tmtz (0.030 g, 0.10 mmol), $Ni(NO_3)_2\cdot 6H_2O$ (0.029 g, 0.10 mmol) and 1,3-H_2bdc (0.017 g, 0.10 mmol) in CH_3OH (5 mL) and H_2O (10 mL) was adjusted to pH 6 with NaOH and then was placed in a Teflon-lined stainless steel vessel, sealed and heated to 110 °C for 24 h, followed by cooling to room temperature at 5 °C h^{-1}. Green crystals of **6** were obtained with a yield of 65% based on tmtz. Anal. Calcd for $C_{32}H_{35}N_9NiO_{4.5}$: C, 56.82; H, 5.22; N, 18.64. Found: C, 56.78; H, 5.18; N, 18.66. IR (cm^{-1}, KBr): 3517w, 3120w, 2920w, 1609s, 1573m, 1536s, 1476w, 1442m, 1384s, 1366s, 1278m, 1207w, 1182w, 1129s, 1071w, 1005w, 990w, 886w, 825w, 742m, 720m, 675m, 652m.

Synthesis of $[Ni(tmtz)(oba)(H_2O)]_n$ (7)

The synthetic procedure was similar to that of **6** except that 1,3-H_2bdc (0.017 g, 0.10 mmol) was replaced by H_2oba (0.026 g, 0.10 mmol). Green crystals of **7** were obtained with a yield of 46% based on tmtz. Anal. Calcd for $C_{30}H_{30}N_6ONiO_6$: C, 57.26; H, 4.81; N, 13.36. Found: C, 57.28; H, 4.78; N, 13.32. IR (cm^{-1}, KBr): 3420m, 3118m, 2929m, 1730W, 1607s, 1551s, 1446m, 1387s, 1278s, 1202w, 1132m, 989m, 876w, 830w, 731m, 665m.

X-ray crystallography

Suitable single crystals of **1–7** were carefully selected under an optical microscope and glued to thin glass fibers. The diffraction data were collected on Rigaku Mercury or Saturn CCD diffractometers with graphite monochromated Mo–Kα radiation. Intensities were collected by the ω scan technique. The structures were solved by direct methods and refined with the full-matrix least-squares technique (SHELXTL-97).[11] The positions of the hydrogen atoms of tmtz and the polycarboxylate ligands were determined with theoretical calculations. The parameters of the crystal data collection and refinement of **1–7** are given in Tables 1 and 2. Selected bond lengths and bond angles are listed in Table S1 in ESI.†

Results and discussion

Description of the crystal structures

$\{[Mn(tmtz)_{0.5}(OH\text{-}bdc)(H_2O)_2]\cdot 2.75H_2O\}_n$ (1). X-ray crystallographic analysis shows that complex **1** exhibits a 1D ladder structure. **1** crystallizes in the triclinic space group $P\bar{1}$. The asymmetric unit of **1** contains one Mn(II) atom, half a tmtz ligand, one OH-bdc ligand, two coordination water molecules and 2.75 lattice water molecules (Fig. S1 in the ESI†). Each Mn(II) ion is six-coordinate with three carboxylate oxygen atoms from two OH-bdc ligands, two oxygen atoms from two water molecules and one nitrogen donor from one tmtz ligand in a distorted octahedral coordination geometry. The Mn(1)–O(2) bond length of 2.456(3) Å is relatively long. The other Mn–O/N bond lengths are in the range of 2.160(4)–2.231(4) Å, which are within the normal distances of those observed in Mn(II)-containing complexes. One carboxylate group (O(1)O(2)) of the OH-bdc ligand acts as a chelating mode and bonds one Mn(II) atom. The other carboxylate group (O3O4) of the OH-bdc ligand acts as a monodentate mode and links one Mn(II) atom. Each tmtz shows an *anti*-conformation, with a dihedral angle of 87.2(2)° between the triazole ring and benzene ring planes.

The Mn(II) atoms are bridged by 2-connected OH-bdc ligands to form a $[Mn(OH\text{-}bdc)]_n$ 1D chain with an Mn···Mn distance of 10.106(3) Å. Two $[Mn(OH\text{-}bdc)]_n$ 1D chains are connected by tmtz ligands to construct a $[Mn(tmtz)(OHbdc)]_n$

Table 1 Crystallographic data for **1–4**

	1	2	3	4
Formula	$C_{16}H_{23.5}MnN_3O_{9.75}$	$C_{32}H_{34}MnN_9O_4$	$C_{24}H_{24}MnN_6O_4$	$C_{30}H_{28}CoN_6O_5$
Fw	468.82	663.62	515.43	611.51
T/K	223(2)	223(2)	293(2)	220(2)
Crystal system	Triclinic	Triclinic	Triclinic	Monoclinic
Space group	$P\bar{1}$	$P\bar{1}$	$P\bar{1}$	$P2_1/n$
a/Å	9.278(3)	10.1259(11)	5.059(2)	12.2271(6)
b/Å	10.106(3)	11.6606(13)	9.540(4)	16.7600(7)
c/Å	12.136(3)	13.7407(13)	11.701(5)	14.4858(6)
α/°	92.828(4)	91.410(3)	90.952(12)	90
β/°	103.413(5)	94.187(3)	91.597(11)	94.476(4)
γ/°	111.715(6)	109.446(3)	100.868(14)	90
V/Å^3	1016.8(5)	1523.7(3)	554.3(4)	2959.5(2)
F(000)	487	692	267	1268
Z	2	2	1	4
ρ_{calcd}/g cm^{-3}	1.531	1.446	1.544	1.372
μ/mm^{-1}	0.707	0.488	0.642	0.629
Reflections collected	9246	14 068	5416	15 618
Unique reflections	4227 (R_{int} = 0.0795)	6853 (R_{int} = 0.0522)	2006 (R_{int} = 0.0703)	6137 (R_{int} = 0.026)
Parameter	298	417	162	383
Goodness of fit	1.082	1.052	1.045	1.011
R_1 [$I > 2\sigma(I)$]	0.0825	0.0707	0.0604	0.0519
wR_2 (all data)	0.1629	0.1732	0.1451	0.1567

Table 2 Crystallographic data for **5–7**

	5	**6**	**7a**	**7b**
Formula	$C_{66}H_{73}Co_4N_{12}O_{28.5}$	$C_{32}H_{35}N_9NiO_{4.5}$	$C_{30}H_{30}N_6NiO_6$	$C_{30}H_{30}N_6NiO_6$
Fw	1726.08	676.40	629.31	629.31
T/K	223(2)	223(2)	223(2)	293(2)
Crystal system	Triclinic	Triclinic	Orthorhombic	Orthorhombic
Space group	$P\bar{1}$	$P\bar{1}$	$P2_12_12_1$	$P2_12_12_1$
a/Å	15.253(3)	10.1205(5)	10.0375(14)	10.121(2)
b/Å	15.285(3)	11.8855(7)	15.2234(18)	15.235(3)
c/Å	18.224(3)	13.4846(7)	18.925(2)	19.027(4)
α/°	107.496(2)	91.532(5)	90	90
β/°	101.147(3)	92.938(4)	90	90
γ/°	112.147(2)	110.081(5)	90	90
V/Å^3	3519.8(11)	1519.71(15)	2891.9(6)	2933.8(10)
F(000)	1778	708	1312	1312
Z	2	2	4	4
ρ_{calcd}/g cm^{-3}	1.629	1.478	1.445	1.425
μ/mm^{-1}	1.023	0.695	0.726	0.715
Reflections collected	28 879	10 574	10 849	13 914
Unique reflections	12 989 (R_{int} = 0.0649)	6198 (R_{int} = 0.0349)	6279 (R_{int} = 0.0446)	4933 (R_{int} = 0.1041)
Parameter	1071	430	399	398
Goodness of fit	1.055	1.030	1.024	1.089
R_1 [$I > 2\sigma(I)$]	0.0833	0.0535	0.0578	0.0887
wR_2 (all data)	0.1909	0.1160	0.1462	0.2054

1D ladder with an adjacent Mn···Mn distance of 13.399(3) Å (Fig. 1a). This ladder adopts a normal arranglement.[12]

The adjacent 1D ladders are held together through versatile hydrogen bond interactions between the OH group, carboxylate group, 2-position nitrogen atoms, coordination water or lattice water molecules to afford a 3D supramolecular framework (Table S2 in the ESI†). There are also π–π stacking interactions between the phenyl rings of the OH-bdc ligand, with a centroid-to-centroid separation of 3.568 Å.[13] These hydrogen bonds and π–π stacking interactions stabilize the 3D supramolecular architecture (Fig. 1b).

[Mn(tmtz)$_{1.5}$(1,3-bdc)]$_n$ (2) and {[Ni(tmtz)$_{1.5}$(1,3-bdc)]·0.5H$_2$O}$_n$ (6). **2** and **6** have a similar 5-connected 2D network. Therefore we only describe the structure of **2** below (Fig. S6 for **6** in the ESI†). **2** crystallizes in the triclinic space group $P\bar{1}$. The asymmetric unit of **2** contains one Mn(II) atom, one and a half tmtz and one 1,3-bdc (Fig. S2 in ESI†). Each

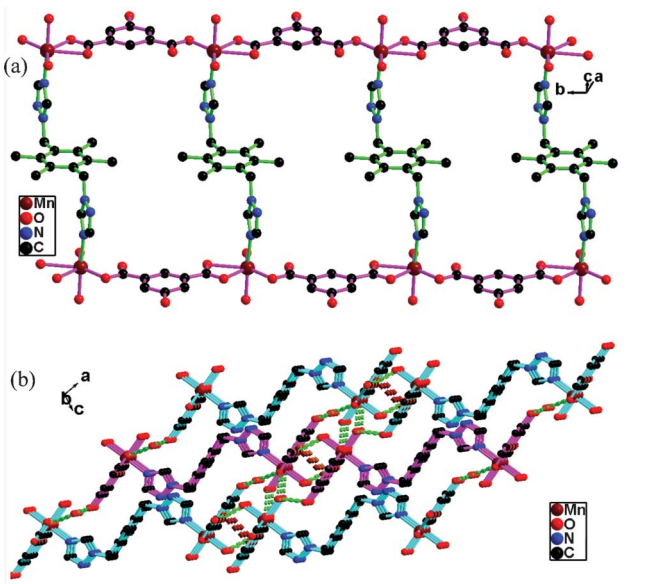

Fig. 1 (a) The 1D ladder in **1**. (b) The 3D supramolecular architecture in **1**. The dark red dashed lines represent the π–π interactions and the bright green dashed lines show the hydrogen bond interactions.

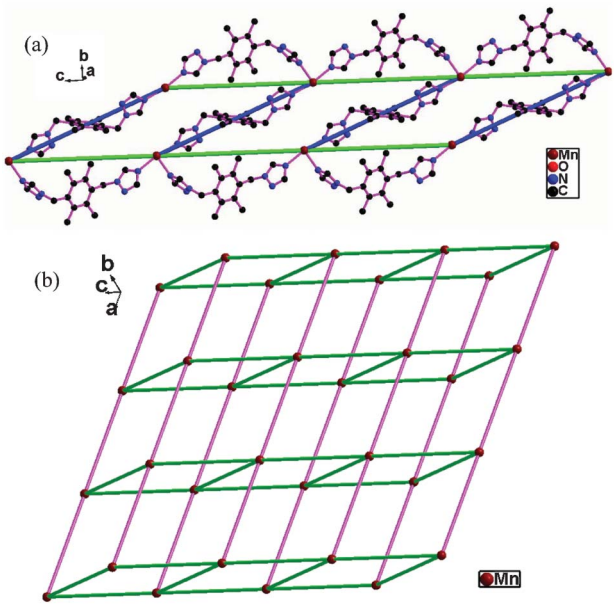

Fig. 2 (a) The [Mn(tmtz)$_{1.5}$]$_n$ 1D ladder in **2**. (b) Schematic plot of the 5-connected 2D network in **2**. The bright green and pink sticks present the tmtz and 1,3-bdc ligands, respectively. The dark red balls show the Mn(II) atoms.

Mn(II) ion is six-coordinate with three carboxylate oxygen atoms from two 1,3-bdc ligands and three nitrogen atoms from three tmtz ligand in a distorted octahedral coordination geometry. The Mn–O/N bond lengths are in the range of 2.112(3)–2.378(3) Å, which are within the normal distances of those observed in Mn(II)-containing complexes.

There are two kinds of tmtz ligands which both show an *anti*-conformation. The dihedral angles between two triazole ring planes, the N(1)–N(3)/C(13)/C(14), N(4)–N(6)/C(15)/C(16) triazole ring plane and the benzene ring planes of one kind of tmtz are 98.6(2), 86.6(2) and 105.2(2)°, respectively. The dihedral angles between the triazole ring and benzene ring planes of the other tmtz is 76.7(2)°. One kind of tmtz ligand (N(1)–N(6)) connects the Mn(II) atoms to generate a $[Mn(tmtz)]_n$ 1D chain with a Mn···Mn separation of 13.741(2) Å. Two adjacent $[Mn(tmtz)]_n$ 1D chains are linked by the other kind of tmtz ligands (N(7)–N(9)) to form a $[Mn(tmtz)_{1.5}]_n$ 1D ladder with a Mn···Mn distance of 16.058(2) Å (Fig. 2a). One carboxylate group (O(1)O(2)) of the 1,3-bdc ligand acts as a monodentate mode. The other carboxylate group (O(3)O(4)) of the 1,3-bdc ligand acts as a chelating mode. Each 1,3-bdc presents a 2-connected bridge and links two Mn(II) atoms, with a Mn···Mn distance of 10.126(2) Å.

Topologically, each Mn(II) atom connects two 1,3-bdc and three tmtz ligands and is 5-connected. The 1,3-bdc and tmtz ligands are 2-connected. Adjacent $[Mn(tmtz)_{1.5}]_n$ 1D ladders are connected by 1,3-bdc bridges to form a 5-connected 2D network (Fig. 2b). The point symbol of the 2D network is $(4^8\cdot6^2)$.[14]

Lee and coworkers synthesized two 5-connected networks.[15] One consists of 5-connected 2D thick layers with $(4^8\cdot6^2)$ topology, which is same as the topology of **2** and **6**. The other exhibits a two-fold interpenetrated 3D bnn topology.

$[Mn(tmtz)(1,4\text{-bdc})]_n$ (3). **3** shows a (4,6)-connected 3D network. **3** crystallizes in the triclinic space group $P\bar{1}$. The asymmetric unit of **3** contains half a Mn(II) atom, half tmtz and half 1,4-bdc (Fig. S3 in the ESI†). Each Mn(II) ion is located in a inversion center and is six-coordinate with four carboxylate oxygen atoms from four 1,4-bdc molecules and two nitrogen atoms from two tmtz ligands in a distorted octahedral coordination geometry. The Mn–O/N bond lengths are in the range of 2.172(3)–2.255(4) Å, which are within the normal distances of those observed in Mn(II)-containing complexes.

Each carboxylate group shows a bidentate bridging mode and connects two Mn(II) atoms. Each 1,4-bdc ligand acts as a 4-connected node and bonds four Mn(II) atoms. Each Mn(II) atom is joined by four 4-connected 1,4-bdc ligands and extends to form a $[Mn(1,4\text{-bdc})]_n$ 2D network with Mn···Mn distances of 5.059(2) and 9.540(4) Å (Fig. 3a).

Each tmtz shows an *anti*-conformation. The dihedral angles between the triazole ring and benzene ring planes of the tmtz is 72.6(2)°. The bidentate tmtz ligands further link the $[Mn(1,4\text{-bdc})]_n$ 2D networks to construct a 3D network (Fig. 3b). Topologically, each Mn(II) atom connects four 1,4-bdc and two tmtz ligands and is 6-connected. The 1,4-bdc ligands are 4-connected and the tmtz ligands are 2-connected. The (4,6)-connected 3D network has fsc topology with a point symbol of $(4^4\cdot6^2)(4^4\cdot6^{10}\cdot8)$.[14,16]

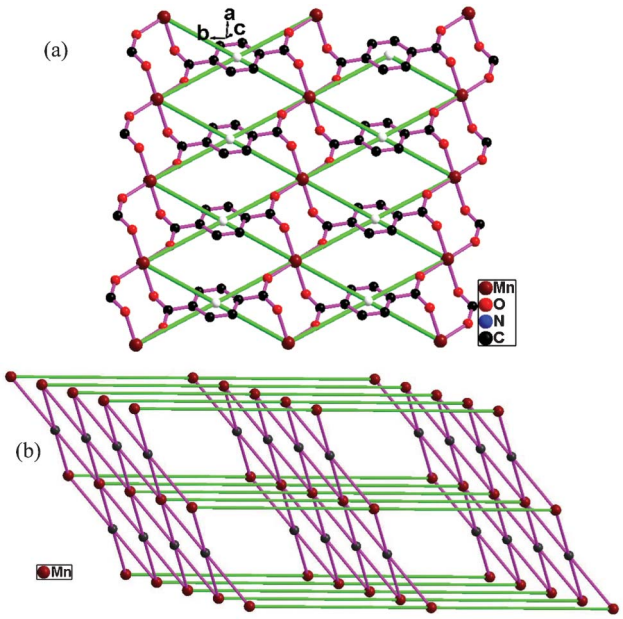

Fig. 3 (a) The $[Mn(1,4\text{-bdc})]_n$ 2D network in **3**. (b) Schematic plot of the (4,6)-connected 3D network in **3**. The dark balls represent the 4-connected 1,4-bdc ligand. The dark red balls show the Mn(II) atoms. The bright green sticks represent the tmtz ligands.

For the (4,6)-connected network, Wen and coworkers synthesized $[Cd(btec)_{0.5}(bimb)_{0.5}]_n$ (H_4btec = 1,2,4,5-benzenetetracarboxylic acid, bimb = 4,4′-bis(1-imidazolyl)biphenyl) with a (4,6)-connected 3D binodal topology, which can be described by a Schläfli symbol of $(4^3\cdot6^3)_2(4^6\cdot6^6\cdot8^3)$ with the vertex symbols for the 4-connected $btec^{4-}$ and 6-connected Cd nodes.[16a] LaDuca and coworkers synthesized $\{[Cu(1,2\text{-phda})(dpa)]3H_2O\}_n$ (1,2-phda =1,2-phenylenediacetate, dpa = 4,4′-dipyridylamine) which possesses a simple (4,4) rhomboid polymeric grid structure but can be considered as a (4,6)-connected binodal supramolecular lattice with $(4^4\cdot6^2)(4^4\cdot6^{10}\cdot8)$ fsc topology.[16b] Lu and coworkers synthesized $[Mn(ptz)Mo_2O_7]$ (ptz = 5-(2-pyridyl)tetrazole) with a (4,6)-connected framework with novel $(3^3\cdot4^2\cdot5)(3^4\cdot4^2\cdot6^2\cdot7^4\cdot8^2\cdot9)(3^4\cdot4^4\cdot5^2\cdot6^4\cdot7)_2$ topology.[16c]

$[Co(tmtz)(oba)]_n$ (4). **4** crystallizes in the monoclinic space group $P2_1/n$. The asymmetric unit consists of one Co(II) atom, one tmtz and one oba (Fig. S4, ESI†). The Co(II) atom is five-coordinate with three carboxylate oxygen atoms from two oba ligands and two nitrogen atoms from two tmtz ligands in a distorted square pyramidal geometry. The Co–O/N bond lengths are in the range of 1.998(2)–2.371(2) Å, which are within the normal distances of those observed in Co(II)-containing complexes. Each tmtz ligand adopts a *gauche*-conformation. The dihedral angles between two triazole ring planes, between the N(1)–N(3)/C(13)/C(14), N(4)–N(6)/C(15)/C(16) triazole ring plane and the benzene ring planes, are 39.1(2), 69.4(2) and 108.5(2)°, respectively. Two *gauche*-conformation tmtz ligands link two Co(II) atoms and form a $[Co_2(tmtz)_2]$ 26-membered cycle with a Co···Co separation of 9.0733(4) Å (Fig. 4a).

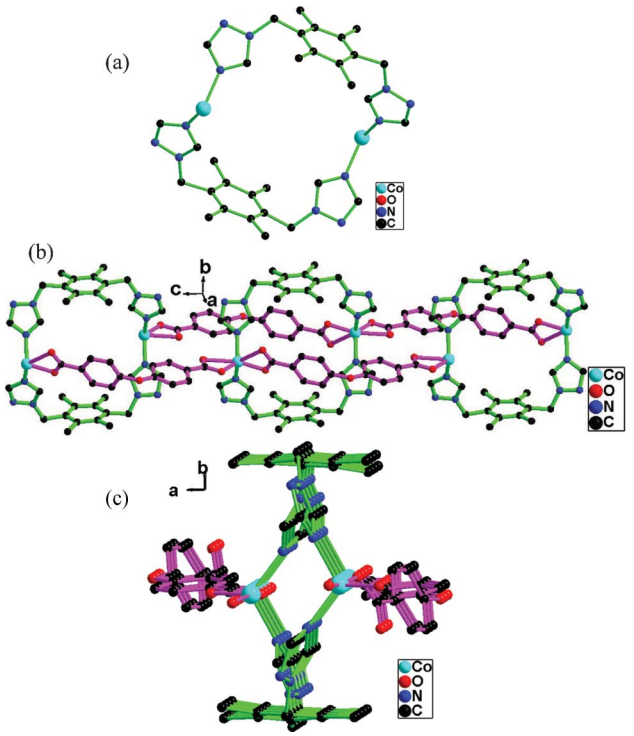

Fig. 4 (a) The $[Co_2(tmtz)_2]$ 26-membered cycle in **4**. (b) Side view of the 1D tubular-like chain in **4**. (c) View of the 1D tubular-like chain along the *c*-axis direction in **4**.

One carboxylate group (O(1)O(2)) of the oba ligand acts as a monodentate mode. The other carboxylate group (O(3)O(4)) of the oba ligand acts as a chelating mode. Each oba acts as 2-connected bridge and links two Co(II) atom with a Co···Co distance of 14.4858(6) Å. Adjacent $[Co_2(tmtz)_2]$ cycles are bridged by two oba ligands to construct a 1D tubular-like chain along the *c*-axis direction (Fig. 4b and 4c). Each 1D tubular-like chain is surrounded by six nearest identical chains (Fig. S4(b) in the ESI†). There are mainly weak van der Waals interactions between the chains. This 1D tubular-like chain is similar to the structures of independent 1D metal–organic nanotubes. A few independent 1D metal–organic nanotubes (MONTs) have been recently reported in the literature.[4a,17]

$\{[Co_4(tmtz)_2(bptc)_2(H_2O)_7]\cdot 3.5H_2O\}_n$ (5). The structure of **5** is a complicated (3,4,4)-connected 3D network. **5** crystallizes in the triclinic space group $P\bar{1}$. The asymmetric unit of **5** contains three Co(II) atoms (Co(1), Co(4), Co(5)), two halves of two Co(II) atoms (Co(2), Co3), one tmtz (N(1)–N(6)), two halves of two tmtz ligands (N(7)–N(9), N(10)–N(12)), two bptc, seven coordination water molecules and three and a half lattice water molecules (Fig. S5 in the ESI†). The Co(1) atom is coordinated by four carboxylate oxygens from two bptc and two nitrogen atoms from two tmtz in a distorted octahedral geometry (Co(1) is 4-connected). Co(2) is located on an inversion center and is six-coordinate with four carboxylate oxygen atoms from two bptc and two oxygen atoms from two water molecules in a distorted octahedral geometry (Co(2) is 2-connected.). Co(3) is located in an inversion center and is six-coordinate with two carboxylate oxygen atoms from two bptc and four oxygen atoms from four water molecules in a distorted octahedral geometry (Co(3) is 2-connected). The Co(4) and Co(5) atoms are coordinated by three carboxylate oxygens from two bptc, two oxygen atoms from two water molecules and one nitrogen atom from one tmtz in a distorted octahedral geometry (Co(4) and Co(5) are 3-connected). All the Co–O/N bond lengths are in the range of 2.046(5)–2.185(4) Å, which are within the normal distances of those observed in Co(II)-containing complexes.

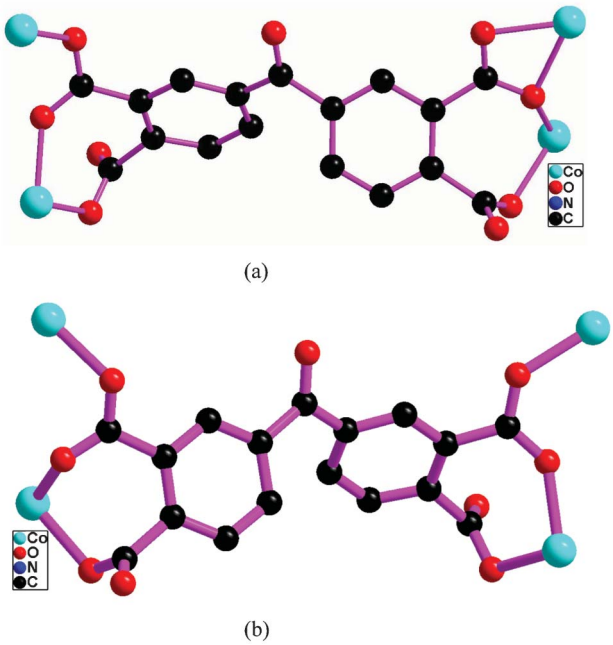

Scheme 3 Two coordination modes of the bptc ligand in **5**.

There are two kinds of bptc ligands (Scheme 3). One carboxylate group (O1O2) of bptc shows a tridentate mode and bridges two Co(II) atoms (Co(1), Co(2)). The other carboxylate group (O5O6) exhibits a bidentate mode and links two Co(II) atoms (Co(4), Co(5)). Another two carboxylate groups (O3O4, O7O8) are monodentate and bond one Co(II) atom (Co(1) or Co(4)). One bptc acts as a 7-dentate mode and connects four Co(II) atoms (Co(1)Co(2)Co(4)Co(5)). Two carboxylate groups (O10O11, O16O17) of the other bptc exhibit a monodentate mode and join one Co(II) atom (Co(1) or Co(5)). Two carboxylate groups (O12O13, O14O15) show a bidentate mode and connect two Co(II) atoms (Co(1)Co(3) or Co(4)Co(5)). The other bptc acts as a 6-dentate mode and connects four Co(II) atoms (Co(1)Co(3)Co(4)Co(5)).

Two kinds of bptc all connect four Co(II) atoms (bptc is 4-connected) and extend to form a $[Co_4(bptc)_2(H_2O)_7]_n$ 2D network (Fig. 5a). There are three kinds of tmtz ligands and all show an *anti*-conformation and a bidentate coordination mode. The dihedral angles between two triazole ring planes, between the N(1)–N(3)/C(13)/C(14), N(4)–N(6)/C(15)/C(16) triazole ring plane and benzene ring planes of one kind tmtz are 14.9(2), 74.5(2) and 60.3(2)°, respectively. The dihedral angle between the N(7)–N(9)/C(23)/C(24) triazole ring and benzene ring planes of the second tmtz is 64.2(2)°. The dihedral angle between the N(10)–N(12)/C(31)/C(32) triazole ring and benzene

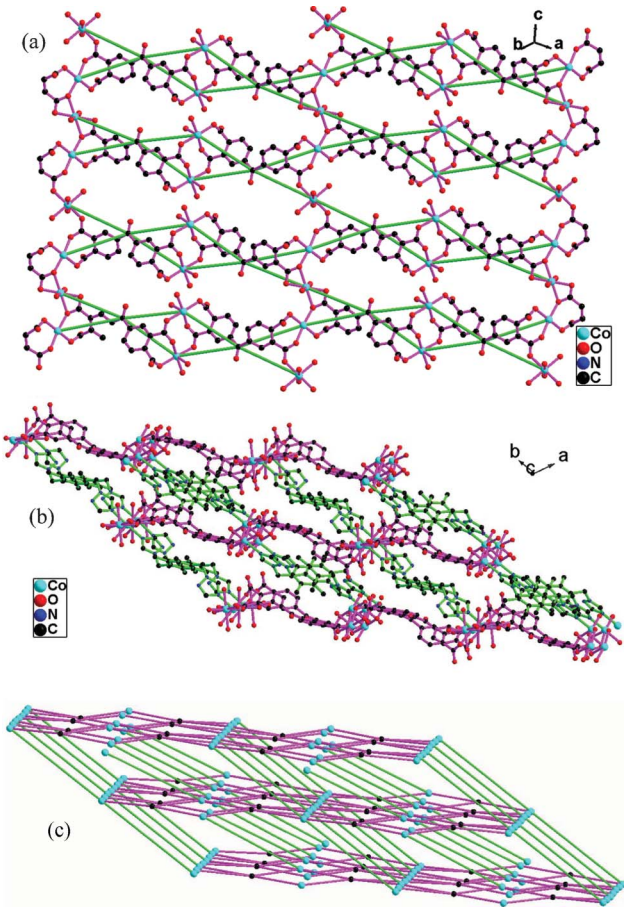

Fig. 5 (a) The $[Co_4(bptc)_2(H_2O)_7]_n$ 2D network in **5**. (b) The (3,4,4)-connected 3D network in **5**. (c) Schematic plot of the (3,4,4)-connected 3D network in **5**. The dark balls represent the 4-connected bptc ligand. The turquoise balls show the Co(II) atoms. The bright green sticks represent the tmtz ligands.

ring planes of the third tmtz is 59.7(2)°. Adjacent $[Co_4(bptc)_2(H_2O)_7]_n$ 2D networks are further linked by tmtz ligands and construct a pillared-layer 3D network (Fig. 5b). In addition, there are rich O–H···O hydrogen bonding interactions which stabilize the network (Table S4 in the ESI†).

Topologically, Co(1) is 4-connected, Co(2) and Co(3) are 2-connected and Co(4) and Co(5) are 3-connected. The bptc ligand is 4-connected and the tmtz ligand is 2-connected. The pillared-layer 3D network is a (3,4,4)-connected 3D network (Fig. 5c). The point symbol of the 3D network is $(4\cdot10\cdot12)_2(4\cdot8^3\cdot10\cdot12)_2(8^2\cdot10^2\cdot12^2)$.[14]

Such a (3,4,4)-connected 3D network is unprecedented to the best of our knowledge. For a (3,4)-connected network, Li and coworkers synthesized an interesting self-catenated coordination framework $[Cd_2(nip)_2(dpa)(H_2O)_3]\cdot2H_2O$ with (3,4)-connected $(4\cdot6^2)_2(4^2\cdot6^2\cdot8^2)$ topology using the V-shaped ligands 5-nitroisophthalic acid (H_2nip) and 4,4′-dipyridylamine (dpa).[18a] $\{Cd(mpda)(biim\text{-}6)_{0.5}(H_2O)\}_n$ (mpda = 1,3-phenylenediacetate, biim-6 = 1,1′-(1,6-hexanedidyl)bis(imidazole)) constructs a (3,4)-connected $(4^2\cdot6^3\cdot8)(4^2\cdot6)$ V_2O_5-type 2D network.[18b]

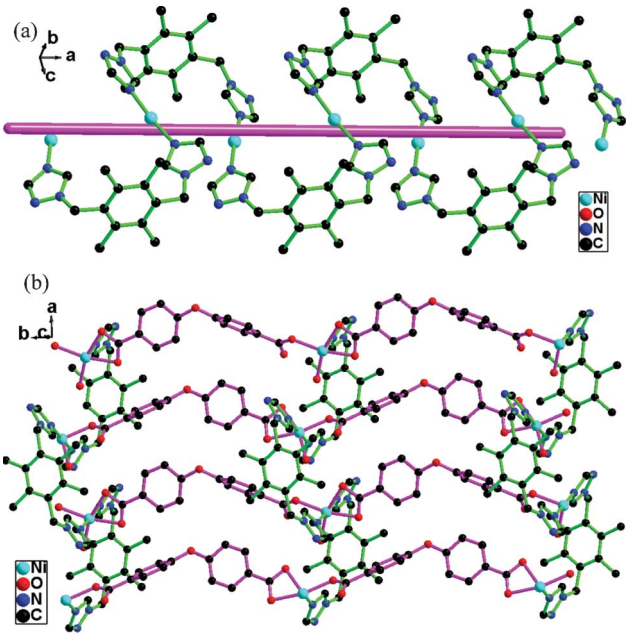

Fig. 6 (a) The $[Ni(tmtz)]_n$ left-handed helical chain in **7a**. (b) The 2D (4.4) network in **7a**.

$[Ni(tmtz)(oba)(H_2O)]_n$ (7). **7a** and **7b** are the enantiomers. Therefore we only describe the structure of **7a** below (Fig. S8 for **7b** in the ESI†). **7a** crystallizes in the chiral orthorhombic space group $P2_12_12_1$ with a Flack parameter of 0.03(2). The asymmetric unit of **7a** contains one Ni(II) atom, one oba and one coordination water. The Ni(II) atom is six-coordinate with three carboxylate oxygen atoms from two oba ligands, one oxygen atom from a coordination water and two nitrogen atoms from two tmtz ligands in a distorted octahedral geometry (Fig. S7a in the ESI†). The Ni–O/N bond lengths are in the range of 2.042(3)–2.119(3) Å, which are within the normal distances of those observed in Ni(II)-containing complexes. Each tmtz ligand adopts a *gauche*-conformation. The dihedral angles between two triazole ring planes, between the N(1)–N(3)/C(13)/C(14), N(4)–N(6)/C(15)/C(16) triazole ring plane and benzene ring planes are 3.6(2), 80.1(2) and 83.6(2)°, respectively. Each *gauche*-conformation tmtz ligand links two Ni(II) atoms and forms a $[Ni(tmtz)]_n$ left-handed helix with a 2_1 screw axis along the *a*-axis with a Ni···Ni distance of 5.2863(10) Å (Fig. 6a).

One carboxylate group (O(1)O(2)) of the oba ligand acts as a monodentate mode. The other carboxylate group (O(3)O(4)) of the oba ligand acts as a chelating mode. Each oba acts as a 2-connected bridge and links two Ni(II) atoms with a Ni···Ni distance of 15.2234(15) Å. Adjacent $[Ni(tmtz)]_n$ helixes are bridged by two oba ligands to form a 2D (4,4) network (Fig. 6b, Fig. S7b in the ESI†).

It should be noted that a chiral assembly demands an efficient transfer of stereochemical information from one helix to the adjacent ones. In this case, the observed chirality of **7a**, as indicated by the $P2_12_12_1$ chiral space group, can be understood in terms of a chirality transfer from the chiral helical chains to the whole framework through the coordina-

tion bonds between the tmtz ligands and helical chains. The stacking plot of **7a** is shown in Fig. S7c in the ESI.†

Comparison of complexes 1–7 and the factors influencing the structure

In complexes **1–7**, flexible tmtz was used as the main ligand, five different polycarboxylate ligands were used as the auxiliary ligands and Mn(II), Co(II) and Ni(II) were the central ions, aiming at exploring the effect of the polycarboxylate and the central metal ions on the assembly and structure of the target complexes. According to the above structural descriptions, the tmtz ligands uniformly behave as bidentate linkers to connect the metal centers in **1–7** but the tmtz ligands adopt an *anti*-conformation in **1**, **2**, **3**, **5** and **6** and a *gauche*-conformation in **4** and **7**.

Initially, we chose OH-bdc as an ancillary ligand and Mn(II) as the central metal ion and thus, a 1D ladder structure of **1** was obtained. When OH-bdc was replaced by 1,3-bdc or Mn(II) was replaced by Ni(II), **2** and **6** with a similar 5-connected 2D network were obtained. The results show that the substitute group of the benzenedicarboxylates has a great effect on the structures. **3** has a (4,6)-connected 3D network with a point symbol of $(4^4\cdot6^2)(4^4\cdot6^{10}\cdot8)$ when 1,3-bdc is replaced by 1,4-bdc. The different structures of **2** and **3** show the influence of the position of the two carboxylate groups on the structures. When a different auxiliary ligand, oba, was used and Co(II) was used as the central metal ion in **4**, a 1D tubular-like chain is synthesized. When a tetracarboxylate ligand bptc was used and Co(II) acts as the central metal ion, a novel complex **5** is synthesized. **5** exhibits a complicated (3,4,4)-connected 3D network with a point symbol of $(4\cdot10\cdot12)_2(4\cdot8^3\cdot10\cdot12)_2(8^2\cdot10^2\cdot12^2)$. When the Co(II) in **4** is replaced by Ni(II), complex **7** with a 2D (4,4) network was synthesized, which crystallizes in a chiral orthorhombic space group $P2_12_12_1$. The different structures of **4** and **7** shows the influence of the central metal ion on the structure. The above results show that the central metal ions, polycarboxylate and flexible triazole co-ligands have a great effect on the formation and the structures of the coordination polymers.

Thermogravimetric analysis

TG experiments (Fig. S9 in the ESI†) were carried out to explore the thermal stability of the seven complexes (see ESI†).

Photoluminescent properties

The d^{10} metal compounds exhibited interesting photoluminescent properties. The solid state luminescence spectra of **1–7** and the free tmtz ligand at room temperature were investigated (Fig. S10 in the ESI†). The free tmtz ligand in the solid state shows an emission band maximum at 310 nm on excitation at 270 nm. The free polycarboxylates OH-H_2bdc, 1,3-H_2bdc and 1,4-H_2bdc exhibit emissions at 361, 370, 390 nm, respectively, according to the literature.[9a] These emission peaks may be assigned to the π^*–n or π^*–π transition, as previously reported. No emission band was observed for **4**, **5** and **7**. **1**, **2**, **3** and **6** present emissions at 355 and 470 nm, 315 and 400 nm, 342 and 430 nm, 313 nm and 400 nm, respectively, upon excitation at 320, 270, 290 and 270 nm. The emissions at 315 nm for **2** and 313 for **6** can be attributed to the ligand tmtz. The emissions 355 nm for **1** and 342 nm for **3** may be attributed to the metal-to-ligand charge-transfer transition (MLCT) (from Mn(II) to tmtz) with a red-shift of 45 nm for **1** and 32 nm for **3**.[9f,19] The emission at 470 nm for **1** may be assigned to MLCT (from Mn(II) to OH-bdc) with a red-shift of 109 nm. The emission at 400 nm for **2** and **6** may be assigned to MLCT (from metal Mn(II) or Ni(II) to 1,3-bdc) with a red-shift of 30 nm. The emission at 430 nm for **3** may be assigned to MLCT (from Mn(II) to 1,4-bdc) with a red-shift of 40 nm.[9f,19]

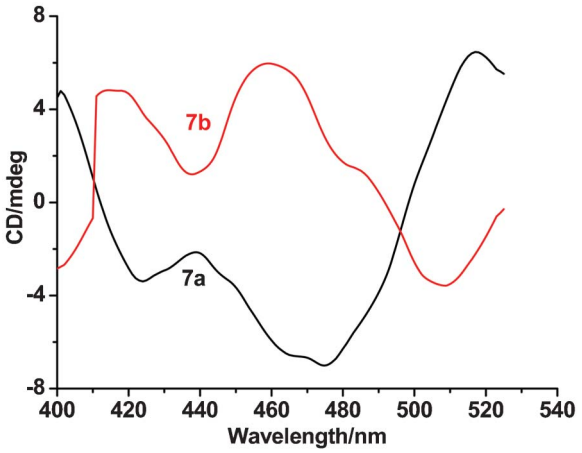

Fig. 7 Solid-state CD spectrum of **7a** and **7b** at room temperature.

CD spectra

In order to confirm the existence of enantiomeric complexes for **7**, solid-state CD spectra were recorded on single crystals of **7** with a KBr disc between 400–525 nm at room temperature. Typically, 80–100 mg of dried KBr and an appropriate amount of the selected crystals were ground extensively in an agate motor and the mixture was pressed as usual. The solid-state CD spectra signals are very sensitive to subtle differences in the thickness and transparency of the disc forms. However, the selected crystals of **7a** and **7b** exhibit opposite Cotton effects at the approximate wavelengths (three peaks at 424, 475 and 517 nm) (Fig. 7), which proves the formation of enantiomeric complexes in the same crystallizations.[9f,20]

Conclusion

In summary, we successfully synthesized seven coordination polymers with the flexible tmtz ligand and five polycarboxylate co-ligands. **1** exhibits a 1D ladder structure. **2** and **6** have a similar 5-connected 2D network. **3** has a (4,6)-connected 3D fsc network. **4** shows a 1D tubular-like chain. **5** exhibits a complicated (3,4,4)-connected 3D network with a point symbol of $(4\cdot10\cdot12)_2(4\cdot8^3\cdot10\cdot12)_2(8^2\cdot10^2\cdot12^2)$. Such a (3,4,4)-connected 3D network is unprecedented to the best of our knowledge. **7** displays a 2D (4,4) network which crystallizes in a chiral orthorhombic space group $P2_12_12_1$. The flexible tmtz ligand can adopt different conformations according to the geometric

needs of the different metal ions. The results indicate that the central metal ions, polycarboxylate and flexible triazole co-ligands have a great effect on the formation and the structures of the coordination polymers.

Acknowledgements

This work was supported by the Natural Science Foundation of China (No. 21171126), the Priority Academic Program Development of Jiangsu Higher Education Institutions and the Funds of Key Laboratory of Organic Synthesis of Jiangsu Province.

References

1 (*a*) S. S. Han and W. A. Goddard III, *J. Am. Chem. Soc.*, 2007, **129**, 8422; (*b*) L. J. Murray, M. Dinca and J. R. Long, *Chem. Soc. Rev.*, 2009, **38**, 1294; (*c*) J. R. Li, R. J. Kuppler and H. C. Zhou, *Chem. Soc. Rev.*, 2009, **38**, 1477; (*d*) J. An, S. J. Geib and N. L. Rosi, *J. Am. Chem. Soc.*, 2010, **132**, 38; (*e*) L. L. Wen, J. B. Zhao, K. L. Lv, Y. H. Wu, K. J. Deng, X. K. Leng and D. F. Li, *Cryst. Growth Des.*, 2012, **12**, 1603; (*f*) Z. Z. Lu, R. Zhang, Y. Z. Li, Z. J. Guo and H. G. Zheng, *J. Am. Chem. Soc.*, 2011, **133**, 4172; (*g*) A. Laguna, T. Lasanta, J. M. Lopez-de-Luzuriaga, M. Monge, P. Naumov and M. E. Olmos, *J. Am. Chem. Soc.*, 2010, **132**, 456; (*h*) C. S. Liu, X. G. Yang, M. Hu, M. Du and S. M. Fang, *Chem. Commun.*, 2012, **48**, 7459; (*i*) P. Yang, X. He, M. X. Li, Q. Ye, J. Z. Ge, Z. X. Wang, S. R. Zhu, M. Shao and H. L. Cai, *J. Mater. Chem.*, 2012, **22**, 2398.

2 (*a*) B. F. Hoskins, R. Robson and D. A. Slizys, *J. Am. Chem. Soc.*, 1997, **119**, 2952; (*b*) B. F. Hoskins, R. Robson and D. A. Slizys, *Angew. Chem., Int. Ed. Engl.*, 1997, **36**, 2336; (*c*) S. Q. Zang, M. M. Dong, Y. J. Fan, H. W. Hou and T. C. W. Mak, *Cryst. Growth Des.*, 2012, **12**, 1239; (*d*) J. Z. Gao, J. Yang, Y. Y. Liu and J. F. Ma, *CrystEngComm*, 2012, **14**, 8173.

3 (*a*) G. Aromí, L. A. Barrios, O. Roubeau and P. Gamez, *Coord. Chem. Rev.*, 2011, **255**, 485; (*b*) J. P. Zhang and X. M. Chen, *Chem. Commun.*, 2006, 1689; (*c*) Y. Garcia, C. Bravic, C. Gieck, D. Chasseau, W. Tremel and P. Gutlich, *Inorg. Chem.*, 2005, **44**, 9723; (*d*) X. Zhu, Y. F. Feng, M. Li, B. L. Li and Y. Zhang, *CrystEngComm*, 2012, **14**, 79; (*e*) M. L. Han, J. G. Wang, L. F. Ma, H. Guo and L. Y. Wang, *CrystEngComm*, 2012, **14**, 2691; (*f*) N. Wang, J. G. Ma, W. Shi and P. Cheng, *CrystEngComm*, 2012, **14**, 5198; (*g*) J. Zhao, D. S. Li, X. J. Ke, B. Liu, K. Zou and H. M. Hu, *Dalton Trans.*, 2012, **41**, 2560.

4 (*a*) X. Zhu, Q. Chen, Z. Yang, B. L. Li and H. Y. Li, *CrystEngComm*, 2013, **15**, 471; (*b*) X. Zhu, X. Y. Wang, B. L. Li, J. Wang and S. Gao, *Polyhedron*, 2012, **31**, 77; (*c*) X. Y. Wang, B. L. Li, X. Zhu and S. Gao, *Eur. J. Inorg. Chem.*, 2005, 3277.

5 (*a*) Y. F. Cui, X. Qian, Q. Chen, B. L. Li and H. Y. Li, *CrystEngComm*, 2012, **14**, 1201; (*b*) Y. F. Cui, P. P. Sun, Q. Chen, B. L. Li and H. Y. Li, *CrystEngComm*, 2012, **14**, 4161.

6 (*a*) J. Wang, X. Zhu, Y. F. Cui, B. L. Li and H. Y. Li, *CrystEngComm*, 2011, **13**, 3342; (*b*) S. Zhao, X. Zhu, J. Wang, Z. Yang, B. L. Li and B. Wu, *Inorg. Chem. Commun.*, 2012, **26**, 37.

7 (*a*) X. Zhu, L. Y. Wang, X. G. Liu, J. Wang, B. L. Li and H. Y. Li, *CrystEngComm*, 2011, **13**, 6090; (*b*) X. Zhu, X. G. Liu, B. L. Li and Y. Zhang, *CrystEngComm*, 2009, **11**, 997.

8 (*a*) X. Zhu, P. P. Sun, J. G. Daing, B. L. Li and H. Y. Li, *Cryst. Growth Des.*, 2012, **12**, 3992; (*b*) B. L. Li, Y. F. Peng, B. Z. Li and Y. Zhang, *Chem. Commun.*, 2005, 2333.

9 (*a*) W. Q. Kan, J. Yang, Y. Y. Liu and J. F. G Ma, *CrystEngComm*, 2012, **14**, 6271; (*b*) H. X. Huang, F. Luo, G. M. Sun, Y. M. Song, X. Z. Tian, Y. Zhu, Z. J. Yuan, X. F. Feng and M. B. Luo, *CrystEngComm*, 2012, **14**, 7861; (*c*) L. Qin, J. S. Hu, M. D. Zhang, Y. Z. Li and H. G. Zheng, *CrystEngComm*, 2012, **14**, 8274; (*d*) H. J. Hao, F. J. Liu, H. F. Su, Z. H. Wang, D. F. Wang, R. B. Huang and L. S. Zheng, *CrystEngComm*, 2012, **14**, 6726; (*e*) M. J. Sie, Y. J. Chang, P. W. Cheng, P. T. Kuo, C. W. Yeh, C. F. Cheng, J. D. Chen and J. C. Wang, *CrystEngComm*, 2012, **14**, 5505; (*f*) Y. Gong, J. Li, J. B. Qin and J. H. Lin, *CrystEngComm*, 2012, **14**, 5862.

10 Y. F. Peng, B. Z. Li, J. H. Zhou, B. L. Li and Y. Zhang, *Chin. J. Struct. Chem.*, 2004, **23**, 985.

11 G. M. Sheldrick, *Acta Crystallogr., Sect. A: Found. Crystallogr.*, 2008, **A64**, 112.

12 (*a*) W. L. Leong and J. J. Vittal, *Chem. Rev.*, 2011, **111**, 688; (*b*) P. Losier and M. J. Zaworotko, *Angew. Chem., Int. Ed. Engl.*, 1996, **35**, 2779; (*c*) L. Carlucci, G. Ciani, S. Maggini and D. M. Proserpio, *Cryst. Growth Des.*, 2008, **8**, 162; (*d*) E. Lee, J. Seo, S. S. Lee and K. M. Park, *Cryst. Growth Des.*, 2012, **12**, 3834.

13 C. Janiak, *J. Chem. Soc., Dalton Trans.*, 2000, 3885.

14 (*a*) V. A. Blatov, M. O'keeffe and D. M. Proserpio, *CrystEngComm*, 2010, **12**, 44; (*b*) E. V. Alexandrov, V. A. Blatov, A. V. Kochetkova and D. M. Proserpio, *CrystEngComm*, 2011, **13**, 3947; (*c*) M. O'Keeffe and O. M. Yaghi, *Chem. Rev.*, 2012, **112**, 675.

15 C. H. Ke and H. M. Ke, *CrystEngComm*, 2012, **14**, 4157.

16 (*a*) L. L. Wen, J. B. Zhao, K. Lv, Y. H. Wu, K. J. Deng, X. K. Leng and D. F. Li, *Cryst. Growth Des.*, 2012, **12**, 1603; (*b*) L. K. Sposato, J. H. Nettleman, M. A. Braverman, R. M. Supkowski and R. L. LaDuca, *Cryst. Growth Des.*, 2010, **10**, 335; (*c*) P. Dong, Q. K. Zhang, F. Wang, S. C. Chen, X. Y. Wu, Z. G. Zhao and C. Z. Lu, *Cryst. Growth Des.*, 2010, **10**, 3218.

17 (*a*) F. N. Dai, H. Y. He and D. F. Sun, *J. Am. Chem. Soc.*, 2008, **130**, 14064; (*b*) Y. B. Dong, Y. Y. Jiang, J. P. Ma, F. L. Liu, J. Li, B. Tang, R. Q. Huang and S. R. Batten, *J. Am. Chem. Soc.*, 2007, **129**, 4520; (*c*) J. Fan, H. F. Zhu, T. Okamura, W. Y. Sun, W. X. Tang and N. Ueyama, *Inorg. Chem.*, 2003, **42**, 158; (*d*) J. Xia, W. Shi, X. Y. Chen, H. S. Wang, P. Cheng, D. Z. Liao and S. P. Yan, *Dalton Trans.*, 2007, 2373; (*e*) S. B. Ren, X. L. Yang, J. Zhang, Y. Z. Li, Y. X. Zheng, H. B. Du and X. Z. You, *CrystEngComm*, 2009, **11**, 246.

18 (*a*) J. Zhao, D. S. Li, Z. Z. Hu, W. W. Dong, K. Zou and J. Y. Lu, *Inorg. Chem. Commun.*, 2011, **14**, 771; (*b*) Y. P. Wu, D. S. Li, J. Zhao, Z. F. Fang, W. W. Dong, G. P. Yang and Y. Y. Wang, *CrystEngComm*, 2012, **14**, 4745.

19 (*a*) Q. Shi, Y. T. Sun, L. Z. Sheng, K. F. Ma, M. L. Hu, X. G. Hu and S. M. Huang, *Cryst. Growth Des.*, 2008, **8**, 3401;

(*b*) R. B. Zhang, Z. J. Li, Y. Y. Qin, J. K. Cheng, J. Zhang and Y. G. Yao, *Inorg. Chem.*, 2008, **47**, 4861; (*c*) N. Wang, J. G. Ma, W. Shi and P. Cheng, *CrystEngComm*, 2012, **14**, 5198.

20 (*a*) S. R. Zheng, S. L. Cai, J. B. Tan, J. Fan and W. G. Zhang, *CrystEngComm*, 2012, **14**, 6241; (*b*) L. Cheng, L. M. Zhang, Q. N. Cao, S. H. Gou, X. Y. Zhang and L. Fang, *CrystEngComm*, 2012, **14**, 7502.